

Test Beam Studies Of 50 μm LGAD sensors.

A. Apresyan^{*,a}, S. Xie^b, C. Pena^b, N. Cartiglia^e, G. Derylo^a, P. Freeman^d,
Z. Galloway^d, H. Al Ghoul^c, L. Gray^a, S. Los^a, N. Minafra^c, C. Royon^c,
H. Sadrozinski^d, A. Seiden^d, M. Spiropulu^b, L. Uplegger^a

^a*Fermi National Accelerator Laboratory, Batavia, IL, USA*

^b*California Institute of Technology, Pasadena, CA, USA*

^c*University of Kansas, KS, USA*

^d*SCIPP, University of California Santa Cruz, CA, USA*

^e*Universit di Torino, Torino, Italy*

Abstract

The high luminosity upgrade of the Large Hadron Collider (HL-LHC) at CERN is expected to provide instantaneous luminosities of $5 \times 10^{34} \text{ cm}^{-2} \text{ s}^{-1}$. The high luminosities expected at the HL-LHC will be accompanied by a factor of 5 to 10 more pileup compared with LHC conditions in 2015, further increasing the challenge for particle identification and event reconstruction. Precision timing allows to extend calorimetric measurements into such a high density environment by subtracting the energy deposits from pileup interactions. Calorimeters employing silicon as the active component have recently become a viable choice for the HL-LHC and future collider experiments which face very high radiation environments. In this article, we present studies of basic calorimetric and precision timing measurements using a prototype composed of tungsten absorber and silicon sensor as the active medium. We show that for the bulk of electromagnetic showers induced by electrons in the range of 20 GeV to 30 GeV, we can achieve time resolutions better than 25 ps per single pad sensor.

Key words:

Silicon, Timing, LGAD

1. Introduction

2. Test-beam Setup

Test-beam measurements were performed at the Fermilab Test-beam Facility (FTBF) which provided a 120 GeV proton beam from the Fermilab Main Injector accelerator. The Devices Under Test (DUTs) were mounted on a remotely operated motorized stage, placed inside the pixel telescope detector [1]. The latter provides better than 10 μm position resolution for charged particles impinging on the DUT. Additionally, a Photek 240

*Corresponding author

Email address: apresyan@fnal.gov (A. Apresyan)

33 microchannel plate photomultiplier tube (MCP-PMT) [2–5] was placed furthest down-
 34 stream, and provided a very precise reference timestamp. Its precision has been previ-
 35 ously measured to be less than 10 psec [4]. A schematic diagram and photograph of the
 36 experimental area are shown in Fig. 1 and Fig. 2, respectively.

37 The DAQ system for the DUTs and the Photek MCP-PMT is based on a CAEN
 38 V1742 digitizer board [6], which provides digitized waveforms sampled at 5 GS/s, and one
 39 ADC count corresponds to 0.25 mV. The CAEN digitizer is voltage- and time-calibrated
 40 using the procedure described in Ref. [7]. The electronic time resolution of the CAEN
 41 V1742 digitizer was measured to be ~ 4 ps, and its impact on the timing measurements
 42 presented in this studies can be neglected. The DAQ for the pixel telescope is based on
 43 the CAPTAN system developed at Fermilab [1]. The track-reconstruction is performed
 44 using the Monicelli software package developed specifically for the testbeam application.

45 The beam is resonantly extracted in a slow spill for each Main Injector cycle delivering
 46 a single 4.2 sec long spill per minute. The primary beam (bunched at 53 MHz) consists
 47 of high energy protons (120 GeV) at variable intensities between 1 and 300 kHz. The
 48 trigger to both the CAEN V1742 and to the pixel telescope was provided by a scintillator
 49 mounted on a photomultiplier tube, placed upstream of the DUTs in the beam-line. Due
 50 to the limited buffer depth of the CAEN V1742 board, special care had to be taken in
 51 the design of the DAQ system to ensure that both the DUT and telescope DAQs collect
 52 exactly the same amount of triggers. This was achieved by limiting the trigger rate by
 53 introducing an adjustable dead-time using a custom-designed FPGA board. We found
 54 that at a rate of about 1,500 triggers per spill the CAEN V1742 and pixel telescope were
 55 maintained fully synchronized. Processed data from the pixel telescope and the DUTs
 56 were merged offline by matching the trigger counters recorded by the two systems.

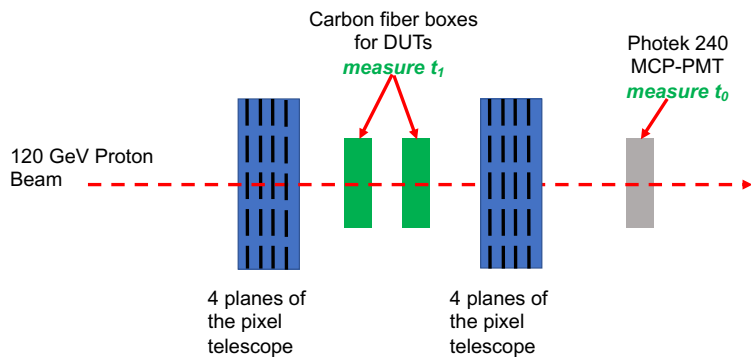


Figure 1: A schematic diagram of the test-beam setup is shown. The t_0 and t_1 are defined in Section 4.

57 The devices under test (DUT) were placed inside the telescope box described in
 58 Ref.[1], and mounted on aluminum mechanical support structure. The telescope box can
 59 be moved remotely in both horizontal and vertical directions, in order to align the DUTs
 60 with the beam. The aluminum support structures for DUT provide both a mechanical
 61 stability for the DUTs, and are equipped with Peltier cooling elements that were used in
 62 this study to operate the DUTs at -10° and -20° C.

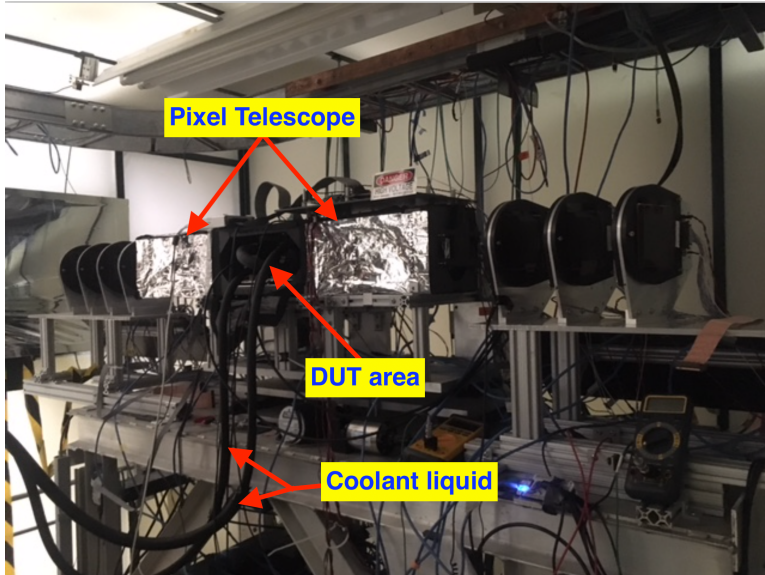


Figure 2: A picture of the experimental area. The pixel telescope detectors are placed inside the ESD shielded boxes on the two sides of the DUT area. Cooling liquid for the Peltier elements inside the DUT area is provided by the two pipes shown in the picture.

63 3. Properties of the tested LGAD sensors

64 Sensors manufactured by Hamamatsu (HPK) and CNM were tested during the test
 65 experiments. All sensors have active thickness of about $50 \mu\text{m}$.

66 **FIXME NICOLO OR HARTMUT: FILL IN DETAILS OF CNM AND**
 67 **HPK SENSORS, PRODUCTION PROCESS ETC** Details on CNM sensors can
 68 be found in Ref. [8, 9]. Hamamatsu sensors have the following properties...

69 Sensors in both single- and four-channel configurations were tested during the mea-
 70 surements. The CNM single-channel sensors had an active area of 1 mm^2 **FIXME: IS**
 71 **THIS CORRECT SIZE OF CNM SINGLE CHANNEL SENSORS?**, and the
 72 HPK single-channel sensors had a diameter of 1 mm. The dimensions of the four channel
 73 sensors from HPK are shown in Fig. 21

74 4. Read-out boards

75 Four boards were used in various measurements presented in this paper, which were
 76 developed at the University of California Santa Cruz (UCSC), University of Kansas (KU),
 77 and at FNAL:

- 78 • A single-channel USCS board that was also used in results presented in Ref. [9]
- 79 • A four-channel USCS readout board
- 80 • A two-channel KU readout board

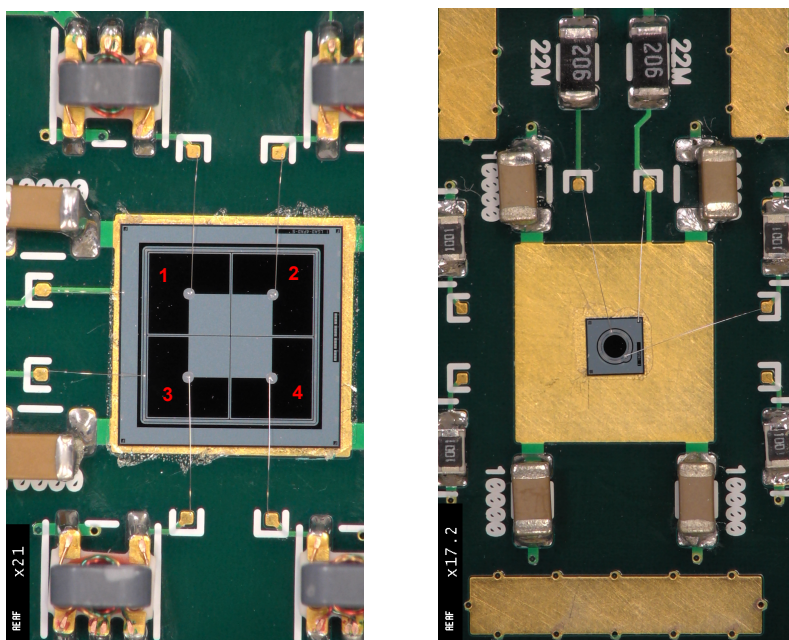


Figure 3: A picture of HPK 50DPix 2x2 array sensor (top), and 50D-GR single sensor (bottom). The pixel labels overlayed on top of the left image are used in the text to identify pixels on the array. Signals from the pixels are read out by the micro-bonds that are connected to the signal pads on the sensors. Signal pads can be seen on the left photograph as four small circles in the center of each pixel.

- 81 • A 4-channel FNAL readout board.

82 and their detailed description is presented below.

83 **FIXME SERGEY** a paragraph describing the FNAL board.

84 **FIXME NICOLA** a paragraph describing the 2-ch KU board.

85 The USCS board 1-channel board is descdibed in details in Ref. [9]. This board
86 uses discrete components and contains several features which allow maintaining a wide
87 bandwidth (~ 2 GHz) and a low noise even in noisy environments. The inverting amplifier
88 uses a high-speed SiGe transistor whcih has a trans-impedance of about 470Ω .

89 **FIXME HARTMUT** a paragraph describing the 4-ch UCSC board.

90 5. Beam test results

91 5.1. Analysis procedure

92 The CAEN digitizer is voltage and time calibrated using the procedure described in
93 Ref. [7]. The time for the reference Photek MCP-PMT detector is obtained by fitting
94 the peak region of the pulse to a Gaussian function and the mean parameter of the
95 Gaussian is assigned as the timestamp t_0 . The time for signals from the LGAD sensors
96 is obtained by performing a linear fit to the rising edge of the pulse and the time at
97 which the pulse reaches 30% of the maximum amplitude is assigned as its timestamp
98 t_1 **FIXME DESCRIBE THE ALGORITHMS FOR LGADS**. We measured the
99 electronic time resolution of the CAEN V1742 digitizer as ~ 4 ps and neglected its impact
100 on the timing measurements described below.

101 Events are required to have a signal in the Photek MCP-PMT consistent with a
102 MIP signal, and a signal above the noise in LGAD sensors. The MIP signal selection in
103 Photek MCP-PMT is the same for all runs, since it was always read out directly by the
104 CAEN digitizer. The signal selection for LGAD boards was optimized for each board
105 individually, by selecting the MIP signal peak fitted with a Landau function.

106 5.2. Study of the uniformity of the LGAD sensors

107 The uniformity of the characteristics of the HPK 50D-PIX sensors was studied using
108 the FNAL readout board. Here, and in the remainder of this article, whenever a scan
109 of a certain characteristic of the array sensors is presented, we show the X-axis scan for
110 pixels 1 and 2, and the Y-axis scan for pixels 1 and 3, as defined on the left picture in
111 Fig. 3. The X-axis scan across pixels 3 and 4, and Y-axis scans across pixels 2 and 4
112 shown qualitatively the same features, and are not shown here.

113 Measurements of the charged particle detection efficiency are shown in Fig. 4. Effi-
114 ciency is defined as the ratio of events that register a signal above the noise level in the
115 LGAD sensor to those that contain a track identified by the pixel telescope pointing at
116 the LGAD sensor. We observe a flat 100% efficiency across the whole sensor area. The
117 left edge of the pixel 1 in Fig. 4 is outside the acceptance of the pixel telescop, hence
118 the efficiency curve does not fully cover its surface. A clear drop in efficiency is observed
119 in the transition region between the two pixels. The area between two pixels is shown
120 in more detail in Fig. 5, and as can be seen, particle detection efficiency is significantly
121 lower in the transition region between the pixels.

122 An important characteristic of the sensors is the unofmity of the signal size across
123 the sensor surface, which directly impacts the timing characteristics of the sensor. The

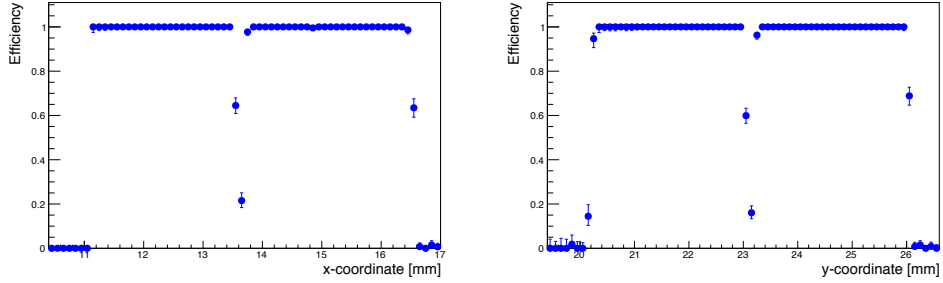


Figure 4: Efficiency measurement across the X- and Y-axes of the HPK 50D-PIX sensor mounted on the FNAL board. The scan of pixels 1 and 2 along the X-axis, and pixels 1 and 3 along the Y-axis is shown, and pixel numbering scheme is defined in Fig. 3.

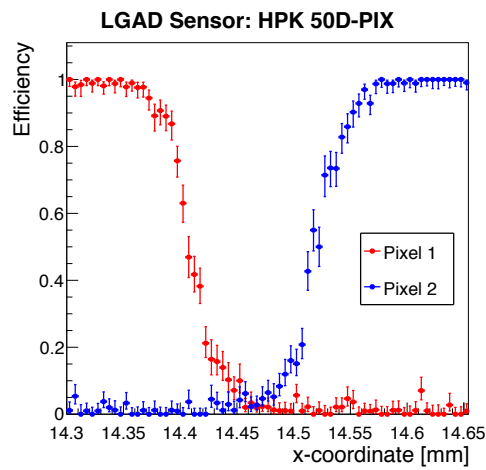


Figure 5: A zoomed version of the efficiency measurement across the X-axis of the HPK 50D-PIX sensor with $10 \mu\text{m}$ binning to show the inter-pixel gap area. Pixel numbering scheme is defined in Fig. 3.

124 distribution of the LGAD signal amplitudes is fit with a Landau distribution, and the
 125 Most Probable Value (MPV) of the fitted function is plotted in Fig. 6. A flat response
 126 with a uniform signal size is observed over the whole sensor area.

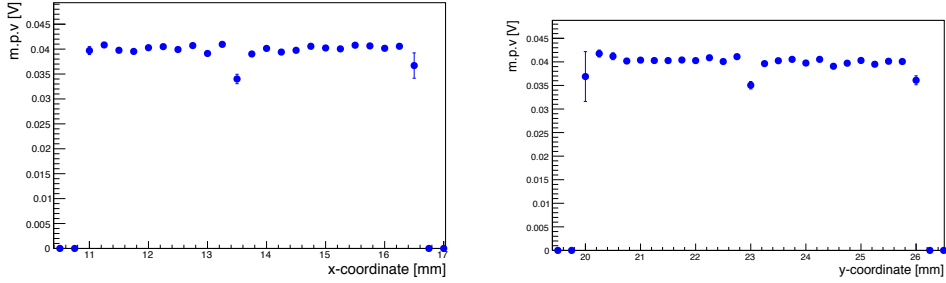


Figure 6: Signal amplitude MPV measurement across the X- and Y-axes of the HPK 50D-PIX sensor mounted on the FNAL board. The scan of pixels 1 and 2 along the X-axis, and pixels 1 and 3 along the Y-axis is shown, and pixel numbering scheme is defined in Fig. 3.

127 The measurement of the time difference between the Photek 240 MCP-PMT time
 128 stamp, and that of the LGAD sensors is shown in Fig. 7. The micro-bonding scheme of
 129 the HPK PIX 2×2 sensors arrays is shown in Fig. 3. The Δt distribution has a distinct
 130 shape where the area under the metalization on top of the sensor shows a shift of about
 131 20 – –30 psec with respect to non-metalized area.

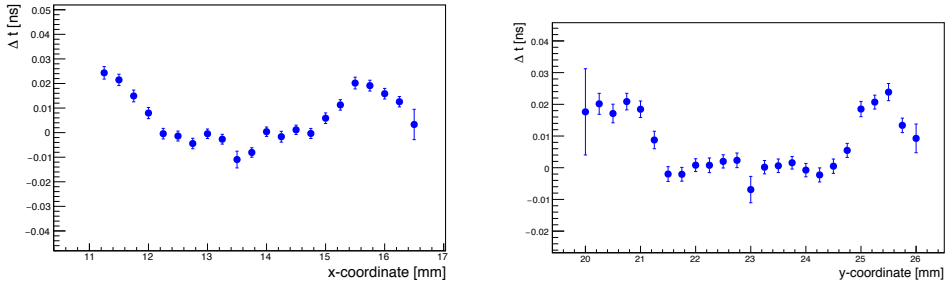


Figure 7: Δt measurement across the X- and Y-axes of the HPK 50D-PIX sensor mounted on the FNAL board. The scan of pixels 1 and 2 along the X-axis, and pixels 1 and 3 along the Y-axis is shown, and pixel numbering scheme is defined in Fig. 3.

132 The measurement of the time resolution scan across the sensor is shown in Fig. 8.
 133 The Δt distribution between LGAD sensor and the Photek 240 MCP-PMT sensor is
 134 fitted with a Gaus function, and its spread σ is referred to in the following as the time
 135 resolution. We observe a uniform time resolution around 40 psec across the whole sensor
 136 area.

137 5.3. Comparison of HPK doping profiles

138 KU boards only, ABCD, time resolution, DeltaT, and MPV plots.

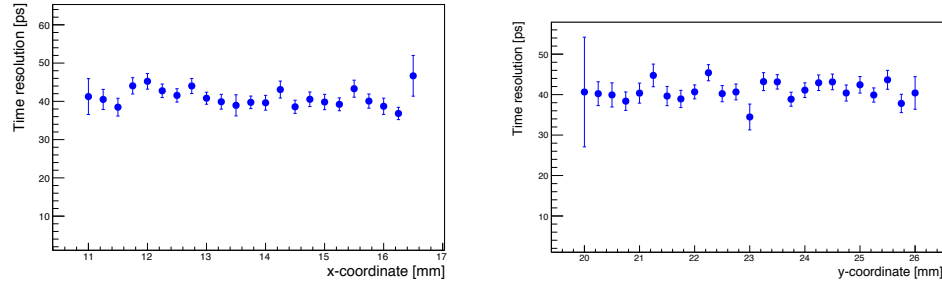


Figure 8: Time resolution measurement across the X- and Y-axes of the HPK 50D-PIX sensor mounted on the FNAL board. The scan of pixels 1 and 2 along the X-axis, and pixels 1 and 3 along the Y-axis is shown, and pixel numbering scheme is defined in Fig. 3.

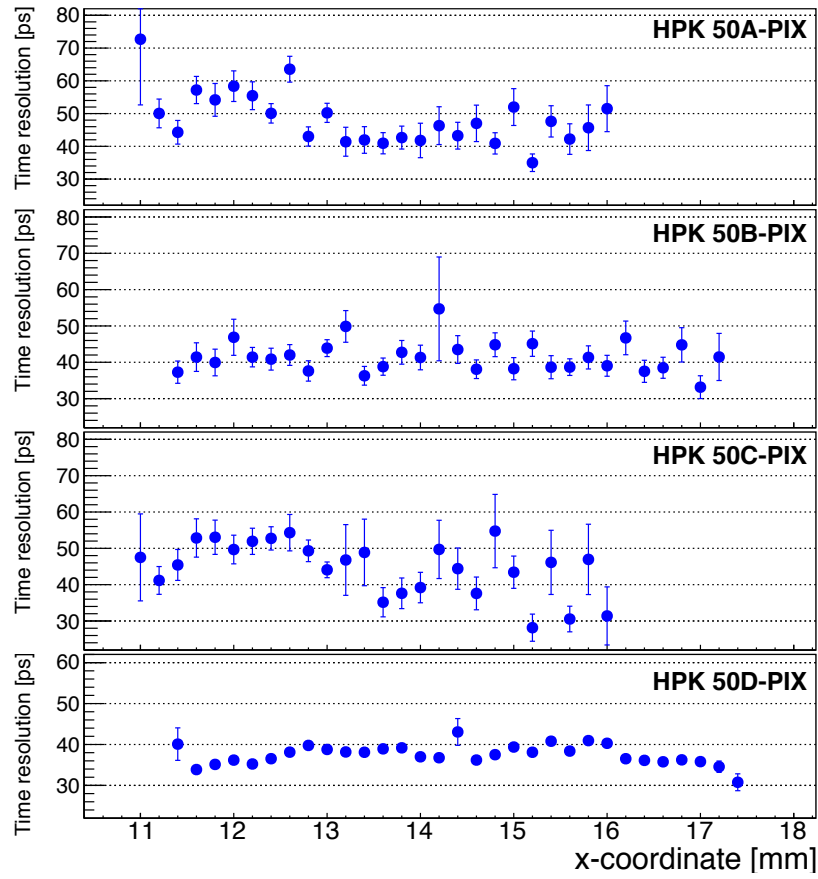


Figure 9: Time resolution on KU board with 50A, B, C, D

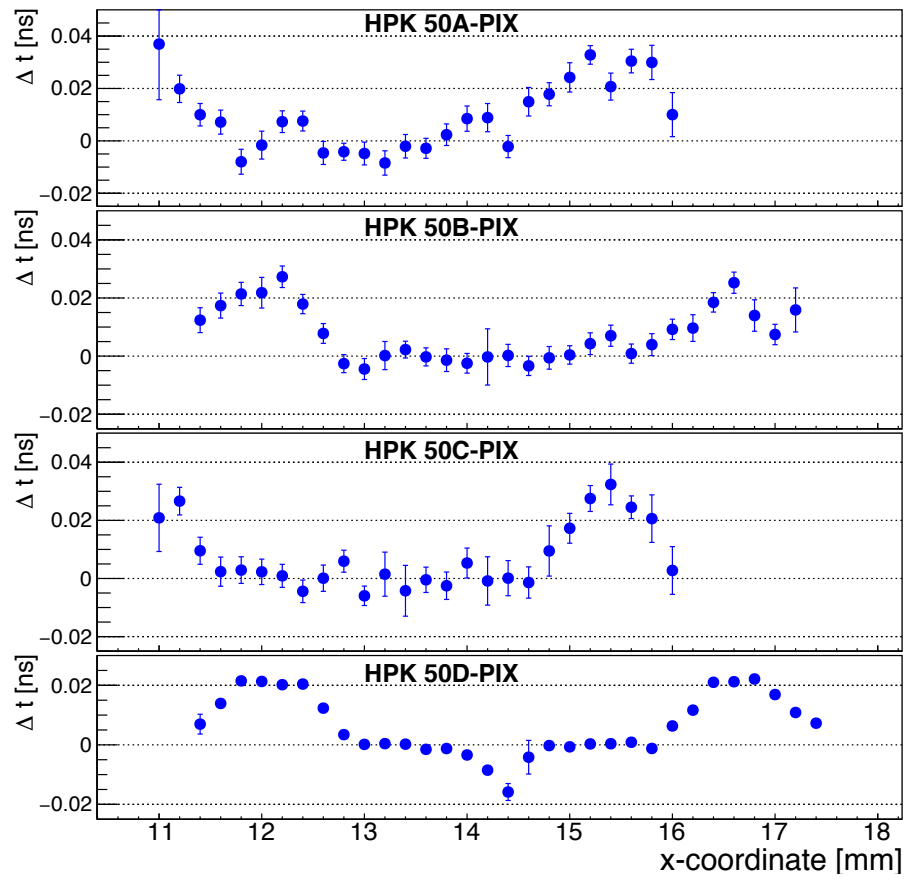


Figure 10: DeltaT on KU board with 50A, B, C, D

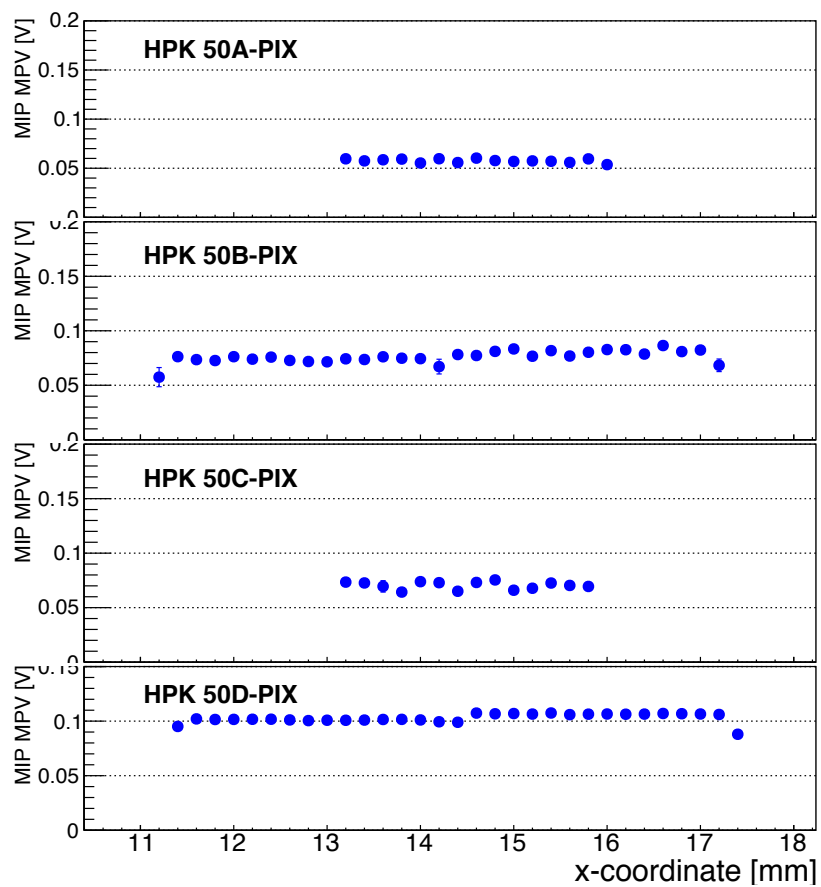


Figure 11: MPV on KU board with 50A, B, C, D

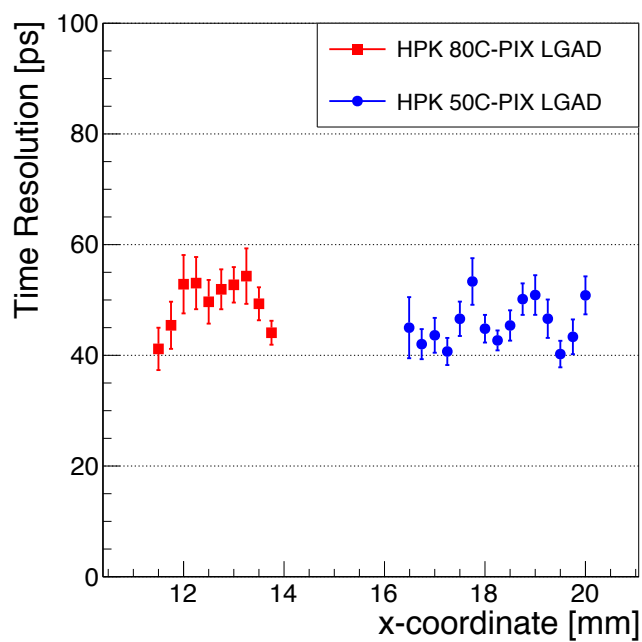


Figure 12: Comparison of time resolution in FNAL 80C versus KU 50C sensors

- ¹³⁹ 5.4. Comparison of HPK 50 μm with 80 μm
¹⁴⁰ 5.5. Temperature dependence of the LGAD sensors

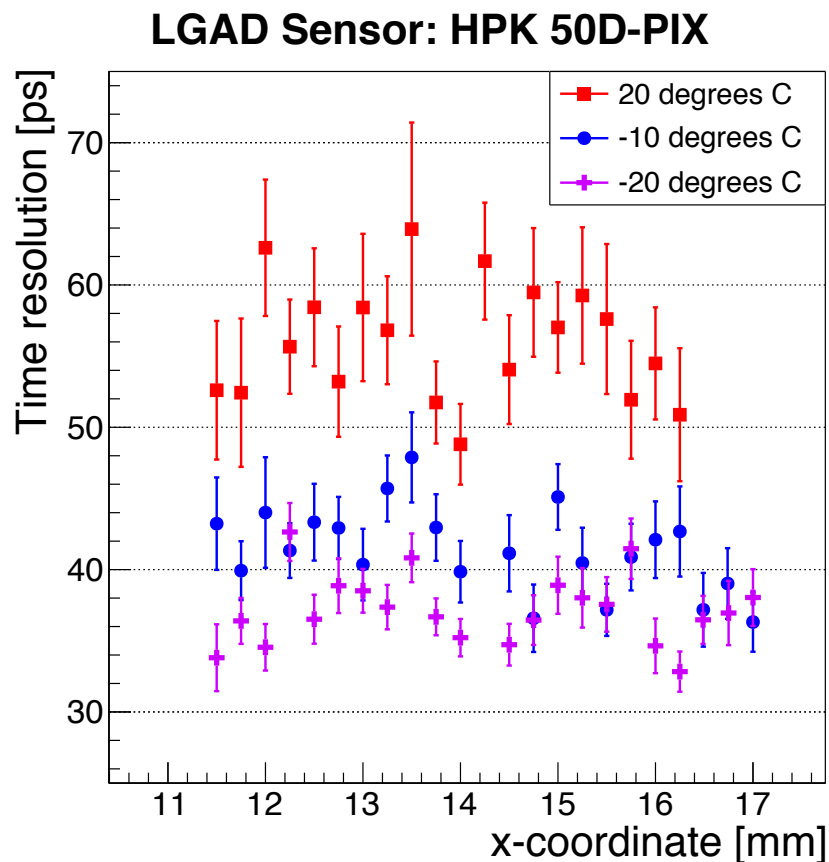


Figure 13: Time resolution on FNAL board with 50D at +20, -10, -20C

- ¹⁴¹ 5.6. Radiation tolerance of the LGADs up to 6×10^{14}

LGAD Sensor: HPK 50D-PIX

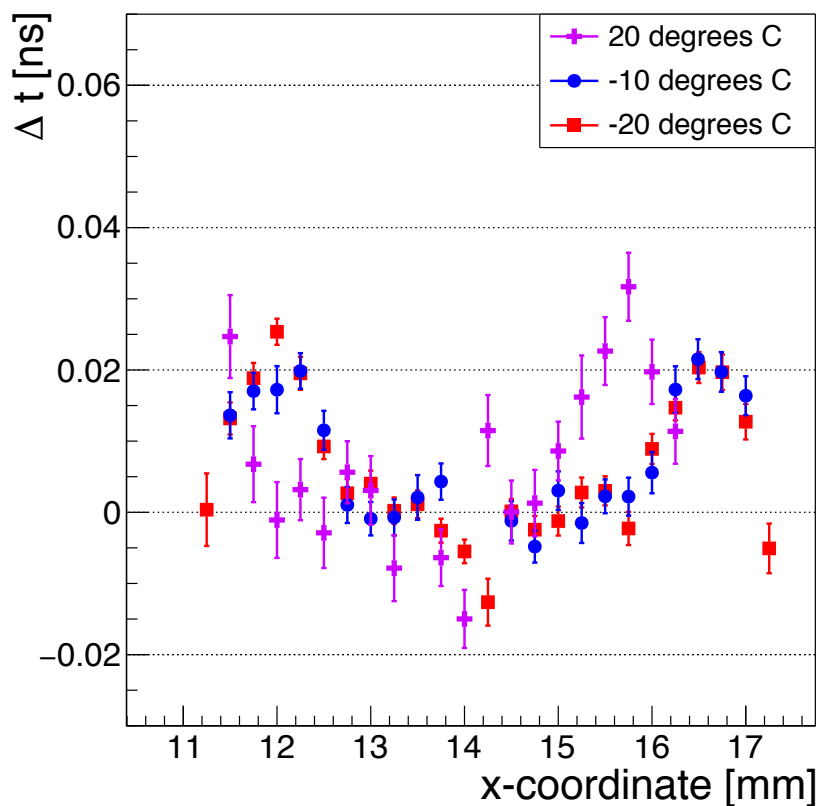


Figure 14: DeltaT on FNAL board with 50D at +20, -10, -20C

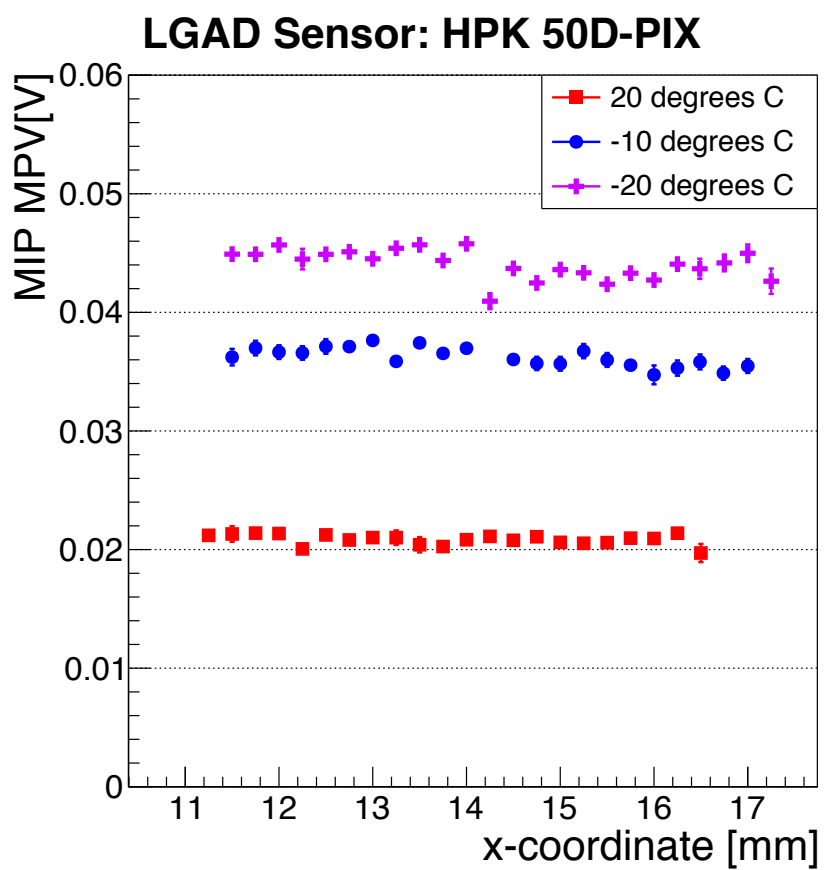


Figure 15: MPV on FNAL board with 50D at +20, -10, -20C

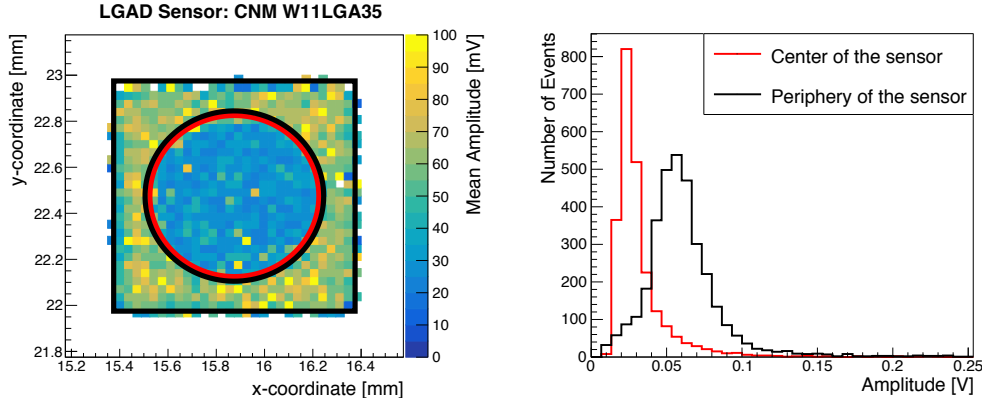


Figure 16: (Left) The map of the amplitude distribution on the irradiated CNM W11LGA35 sensor across X and Y coordinates. Two distinct regions on the sensor surface can be identified according to the amplitude distribution: the center of the sensor (area within the red circle), and the periphery of the sensor (area between the black circle and black square). (Right) Amplitude distribution in the two areas of the irradiated CNM W11LGA35 sensor.

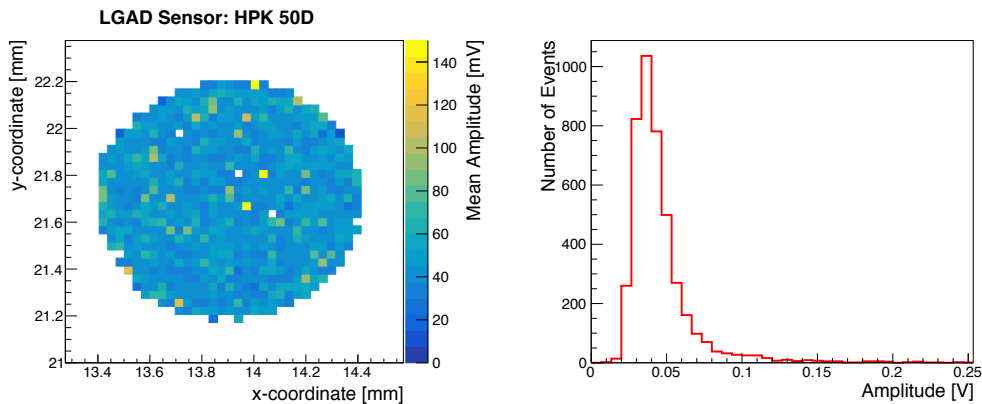


Figure 17: (Left) The map of the amplitude distribution on the irradiated HPK 50D sensor across X and Y coordinates. Two distinct regions on the sensor surface can be identified according to the amplitude distribution: the center of the sensor (area within the red circle), and the periphery of the sensor (area between the black circle and black square). (Right) Amplitude distribution in the two areas of the irradiated HPK 50D sensor.

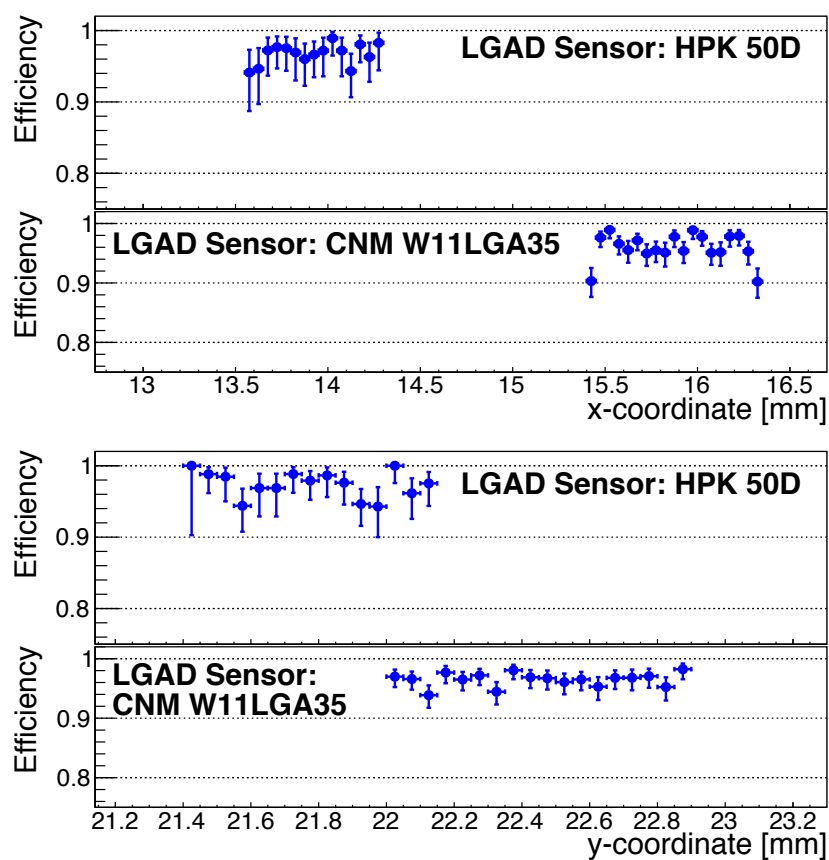


Figure 18: Efficiency vs X and Y on CNM and HPK irradiated

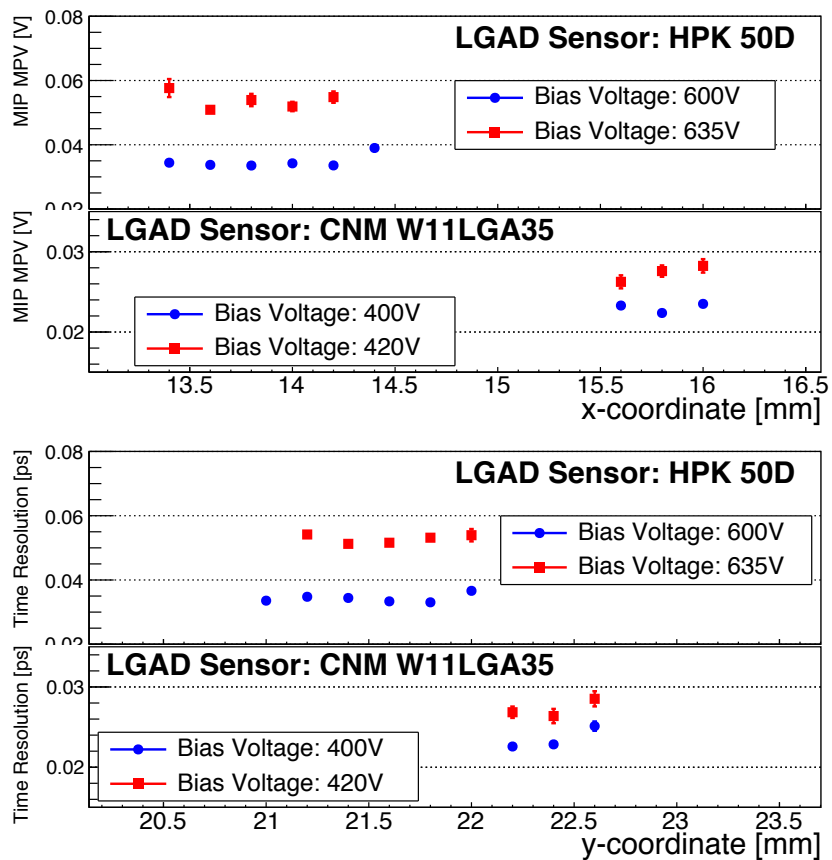


Figure 19: MPV vs X and Y on CNM and HPK irradiated

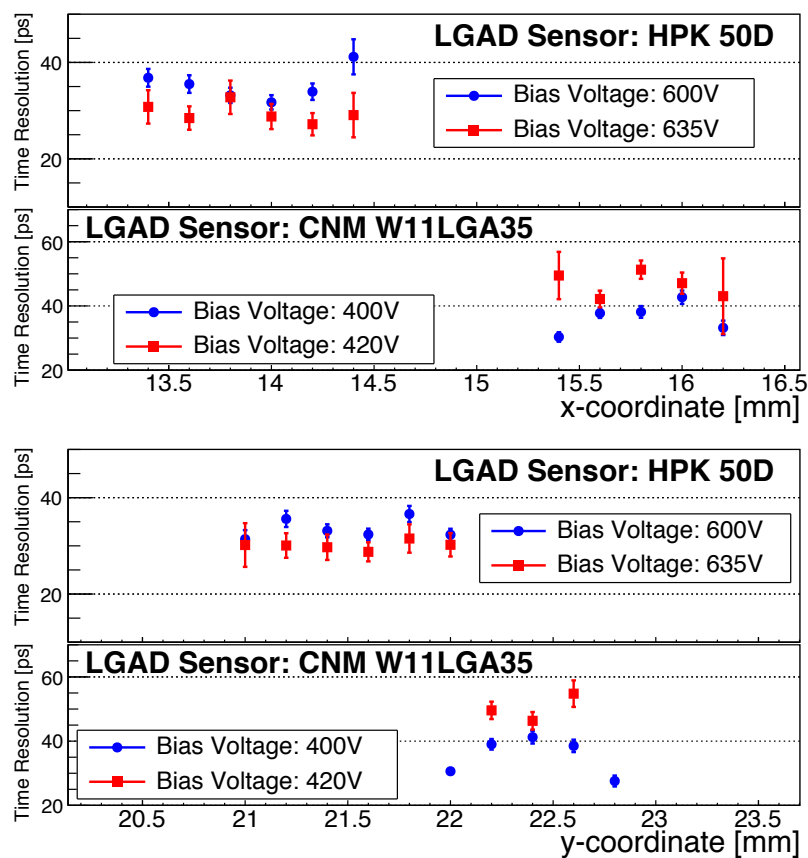


Figure 20: Time Resolution vs X and Y on CNM and HPK irradiated

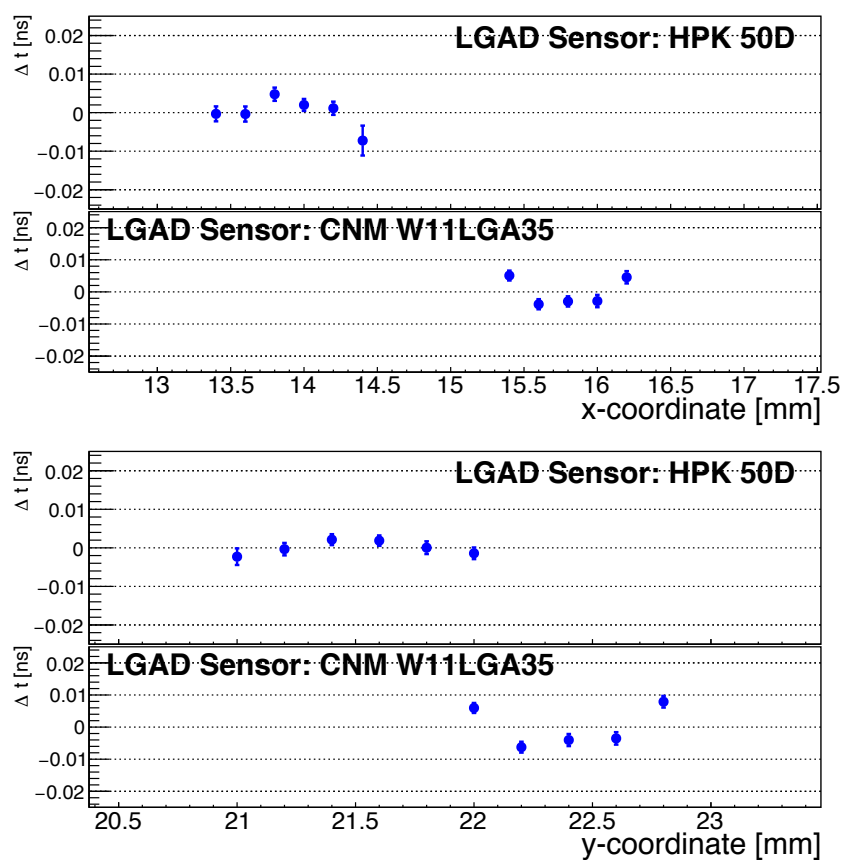


Figure 21: DeltaT vs X and Y on CNM and HPK irradiated

¹⁴² **6. Conclusion**

¹⁴³ All is good!

¹⁴⁴ **Acknowledgement**

¹⁴⁵ We would like to thank Alan Prosser and Ryan Rivera for their critical help in setting
¹⁴⁶ up the DAQ and trigger chain.

¹⁴⁷ **References**

- [1] S. Kwan, C. Lei, D. Menasce, L. Moroni, J. Ngadiuba, A. Prosser, R. Rivera, S. Terzo, M. Turquetti, L. Uplegger, L. Vigani, and M. E. Dinardo, “The pixel tracking telescope at the fermilab test beam facility,” *Nuclear Instruments and Methods in Physics Research Section A: Accelerators, Spectrometers, Detectors and Associated Equipment*, vol. 811, pp. 162 – 169, 2016.
- [2] D. Anderson, A. Apresyan, A. Bornheim, J. Duarte, C. Pena, A. Ronzhin, M. Spiropulu, J. Trevor, and S. Xie, “On Timing Properties of LYSO-Based Calorimeters,” *Nucl. Instrum. Meth. A*, vol. 794, pp. 7–14, 2015.
- [3] A. Ronzhin, S. Los, E. Ramberg, M. Spiropulu, A. Apresyan, S. Xie, H. Kim, and A. Zatserklyaniy, “Development of a new fast shower maximum detector based on microchannel plates photomultipliers (MCP-PMT) as an active element,” *Nucl. Instrum. Meth. A*, vol. 759, pp. 65 – 73, 2014.
- [4] A. Ronzhin, S. Los, E. Ramberg, A. Apresyan, S. Xie, M. Spiropulu, and H. Kim, “Study of the timing performance of micro-channel plate photomultiplier for use as an active layer in a shower maximum detector,” *Nucl. Instrum. Meth. A*, vol. 795, pp. 288 – 292, 2015.
- [5] A. Ronzhin, S. Los, E. Ramberg, A. Apresyan, S. Xie, M. Spiropulu, and H. Kim, “Direct tests of micro channel plates as the active element of a new shower maximum detector,” *Nucl. Instrum. Meth. A*, vol. 795, pp. 52 – 57, 2015.
- [6] <http://www.caen.it/cssite/CaenProd.jsp?parent=11&idmod=661>.
- [7] H. Kim, C.-T. Chen, N. Eclov, A. Ronzhin, P. Murat, E. Ramberg, S. Los, W. Moses, W.-S. Choong, and C.-M. Kao, “A new time calibration method for switched-capacitor-array-based waveform samplers,” *Nucl. Instrum. Meth. A*, vol. 767, pp. 67 – 74, 2014.
- [8] M. Carulla et al, “First 50 m thick LGAD fabrication at CNM.” <https://agenda.infn.it/getFile.py/access?contribId=20&sessionId=8&resId=0&materialId=slides&confId=11109>, 2016. 28th RD50 Workshop, Torino.
- [9] N. Cartiglia *et al.*, “Beam test results of a 16 ps timing system based on ultra-fast silicon detectors,” *Nucl. Instrum. Meth. A*, vol. 850, pp. 83 – 88, 2017.